PASSIVE THERMAL MANAGEMENT FOR A FUEL CELL REFORMING PROCESS

David B. Sarraf [*] and Richard W. Bonner.[†]
[1]*Advanced Cooling Technologies, Inc., Lancaster, PA 17601*

Denis Colahan [‡]
Naval Surface Warfare Center, Philadelphia, PA

The US Navy is investigating hydrogen fuel cells powered by reformed naval logistic diesel fuel as a means of providing distributed ship service electrical power. Operation on diesel fuel requires a reformer system to remove sulfur and convert the synthesis gas into a hydrogen rich stream. Temperature control of the reformer system is made difficult because rapid changes in the fuel cell electrical load require rapid changes in the reactant flow rate. The current valve-based control system has several drawbacks, including increased system volume and pressure drop and decreased reliability. A heat exchanger based on Variable Conductance Heat Pipes (VCHP-HX) is currently under development. The VCHP-HX can passively regulate reactant temperature without a control valve and its attendant disadvantages. This paper presents the results to date of a VCHP-HX development program, including compatibility testing of candidate working fluid and wall materials, test data from a single VCHP, and test results from an array of VCHPs operating at reduced temperature. Suitable working fluids have been identified and the test results show good agreement with model predictions.

Nomenclature

A_1 = surface area of heat pipe evaporator
A_2 = surface area of heat pipe condenser not covered by noncondensable gas
$C_{P,1}$ = heat capacity of process stream
$C_{P,2}$ = heat capacity of steam stream
h_1 = effective heat transfer coefficient on heat pipe evaporator surface, including fin efficiency effects
h_2 = effective heat transfer coefficient on heat pipe condenser surface, including fin efficiency effects
H_1 = height of heat exchanger duct on process side
H_2 = height of heat exchanger duct on steam side
n_{ncg} = moles of noncondensable gas in heat pipe
P_{sat} = saturation pressure of working fluid in heat pipe
R = ideal gas constant
t = time
T_1 = temperature of process stream
T_2 = temperature of steam stream
T_{HP} = heat pipe temperature
T_{ncg} = noncondenable gas temperature
U = overall heat transfer coefficient based on the tube sheet area, accounting for fin efficiency effects as well as changes in local noncondensable gas position in condenser
V_c = volume of heat pipe condenser
V_R = volume of heat pipe reservoir

[*] Senior Engineer, 1046 New Holland Ave., Lancaster PA 17601, AIAA Member
[†] Project Engineer, 1046 New Holland Ave., Lancaster PA 17601
[‡] Senior Engineer Machinery Research, Naval Surface Warfare Center, 1000 Kitty Hawk Ave., Philadelphia, PA 19112

x = heat exchanger position
ρ_1 = density of process stream
ρ_2 = density of steam stream
v_1 = velocity of process stream
v_2 = velocity of steam stream

VHCP = Variable Conductance Heat Pipe
LTS = Low Temperature Shift
HTS = High Temperature Shift
NCG = Non-condensable Gas

I. Introduction

The Navy is investigating hydrogen fuel cells powered by reformed naval logistic diesel fuel as a means of providing distributed ship service electrical power.[1] The primary advantages of fuel cells include high reliability due to the lack of moving parts and the potential of up to 50% thermal efficiency partially due to the ability to effectively utilize waste heat.[2] Hydrogen fuel cell operation using diesel fuel requires a reforming process to remove sulfur and steam reform the diesel fuel into a hydrogen rich stream.[3] A typical reformer system is shown in Figure 1. Diesel fuel and air enter the system at the left. The fuel is first desulfurized. Steam, air and diesel fuel react in a High Temperature Shift (HTS) and a Low Temperature Shift (LTS) reactor to produce as much hydrogen as possible. Hydrogen is then separated from the undesirable carbon products (CO, CO_2) before oxidation in the fuel cell. The steam needed for the steam reforming process is generated by heat removed from the reactant streams. Three heat exchangers move heat from the gas stream into the steam drum, where feedwater is changed to saturated steam. The superheater recovers heat from the first reactor and further heats the steam.

The operating temperature of the reactors must be closely controlled to maintain their chemical equilibrium. Temperature control is made more difficult than typical reforming systems because changes in the fuel cell electrical load and the resulting changes in reactant flow rates occure more frequently and drastically. The system shown in Figure 1 must maintain inlet and outlet temperatures within ±30°C despite a turndown ratio of 5:1 in reactant flow rate. A robust control scheme is needed to control the reactor temperatures within operational limits over all anticipated reactant flow rates.

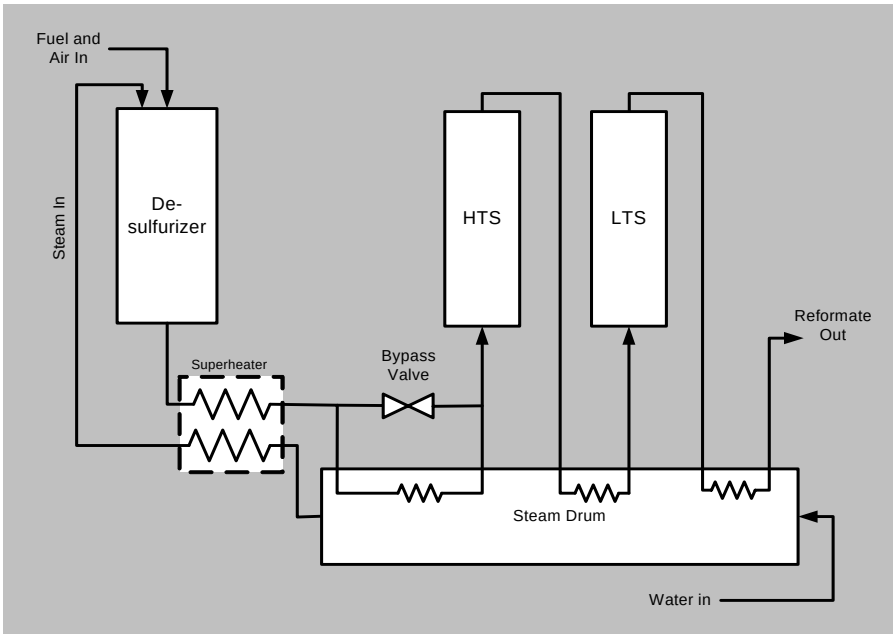

Figure 1 Reformer Schematic

The current means of temperature control is the bypass valve between the superheater and the HTS reactor. of the valve controls the amount of by-pass flow around the first heat exchanger. As the reactant flow decreases, the valve opens to route less of the reactants through the exchanger. Less heat is removed from the gas stream and the average gas temperature entering the reactor rises. As reactant flow increases, the valve closes. Flow through the exchanger is increased, more heat is removed from the gas stream, and the average gas temperature entering the reactor falls. By actively changing the valve position in response to reactant flow and fuel cell output, the temperature of the gas stream and the reactor can be kept stable despite wide changes in flow rate.

Although the valve-based system works, it has several drawbacks. A valve-based system requires active control. Power is needed to drive the valve, and a feedback means is needed to compute valve position. Another drawback is pressure drop. For the valve to provide sufficient bypass flow and an acceptable turndown ratio, the valve must be physically large or the heat exchanger must have a larger-than-normal pressure drop. Integration is another problem. The valve-based system does not lend itself to a proposed in-line reformer system where the reactors are all collinear or close-coupled. Finally, the valve reduces reliability. The valve and the control system are additional components that consume space and are subject to failure.

Heat pipes transport heat by two phase flow of a working fluid.[4] Shown in Figure 2, a heat pipe is a vacuum tight device consisting of a working fluid and a wick structure. The heat input vaporizes the liquid working fluid inside the wick in the evaporator section. The saturated vapor, carrying the latent heat of vaporization, flows towards the colder condenser section. In the condenser, the vapor condenses and gives up its latent heat. The condensed liquid returns to the evaporator through the wick structure by capillary action. The phase change processes and two-phase flow circulation continue as long as the temperature gradient between the evaporator and condenser are maintained.

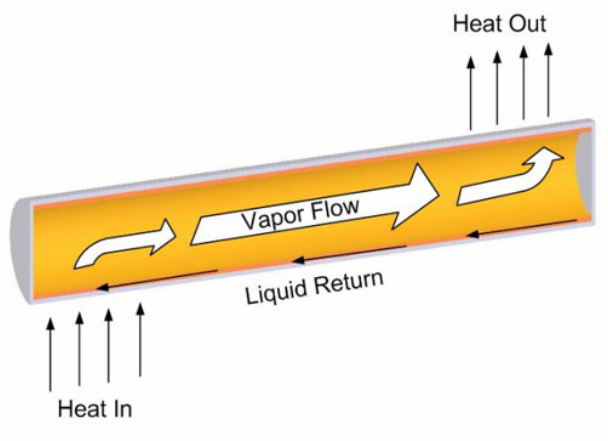

Figure 2 Heat Pipe Operation

Variable Conductance Heat Pipes, or VCHPs, can passively maintain a relatively constant evaporator temperature over a wide range of input powers.[5,6,7] Shown in Figure 3, a VCHP is similar to a conventional heat pipe but has a reservoir and controlled amount of non-condensable gas (NCG). When the heat pipe is operating, the gas is swept toward the condenser end of the heat pipe by the flow of the working fluid vapor. The NCG then blocks the working fluid from reaching a portion of the condenser. The VCHP works by varying the amount of condenser available to the working fluid. As the evaporator temperature increases, the vapor temperature rises, the NCG compresses (Fig 3 top), and more condenser is exposed to the working fluid. This increases the effective thermal conductivity of the heat pipe and drives the temperature of the evaporator down. Conversely, if the evaporator cools, the vapor pressure drops and the NCG expands (Fig 3 bottom). This reduces the amount of available condenser, decreases the heat pipe thermal conductivity, and drives the evaporator temperature up.

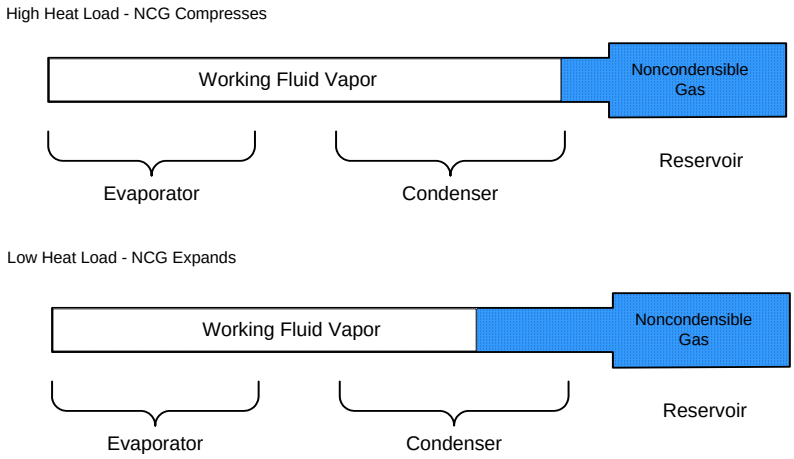

Figure 3 VCHP Operation

For the simple VCHP shown in Figure 3, the degree of control depends primarily on two factors: the slope of the working fluid vapor pressure curve, and the ratio of reservoir and condenser volumes. Working fluids having steeper vapor pressure curves at the particular operating temperature result in tighter temperature control. Small changes in temperature result in large changes in pressure and subsequently large changes in the NCG volume. Similarly, large reservoir volumes improve control because a given pressure change results in a larger change in the position of the gas/vapor interface in the condenser. Smaller reservoirs contain less gas and can provide less change in the position of the gas/vapor interface. Typical turndown ratios of between 5:1 and 10:1 are possible depending upon reservoir size. Temperature control can be as close as ±3°C for some combinations of working fluid and operating temperature.

A simple VCHP heat exchanger is shown in Figure 4. Heat is absorbed from the reactant stream by the lower set of plate fins. Heat is conducted into the heat pipe and transported through the tube sheet to the upper set of fins. There, the heat is absorbed by the coolant stream. An actual exchanger would be constructed of an array of heat pipes. The fluid streams would be contained by simple boxes or plenums built around the fin stacks. The boxes could be brazed or welded to the tube sheet to form a hermetic structure, or the fin stacks and tube sheets could be captured between a pair of shells much like a conventional tube-and-shell heat exchanger. One possible enhancement would be the use of a double-wall tube sheet. That would provide additional isolation between the fluid streams because two joints would need to be breached before a leak occurred. The volume between the two sheets could serve as a tell-tale volume that would provide warning when one of the two joints was breached.

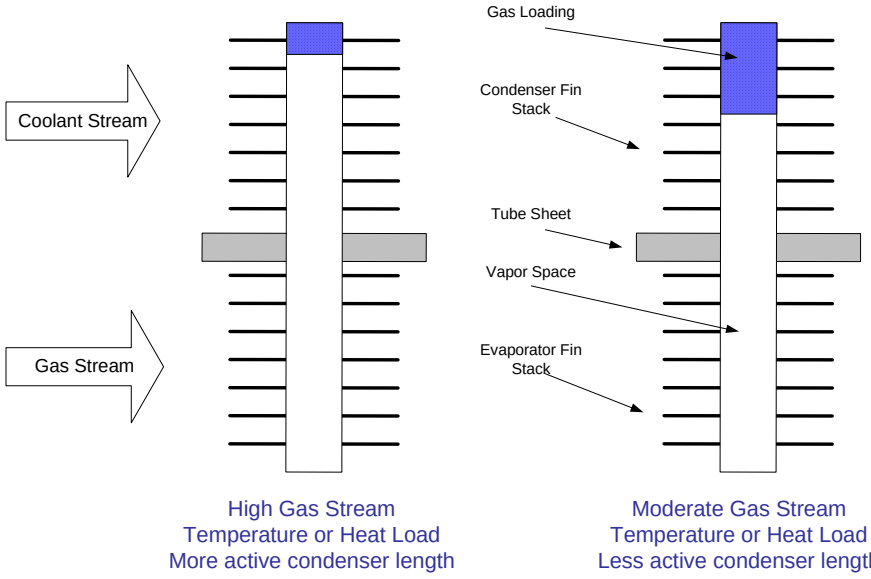

Figure 4: VCHP Heat Exchanger Schematic

A VCHP Heat Exchanger provides several significant advantages over the current valve-based scheme. It requires no additional control systems, sensors, actuators, or external power for operation, which makes it intrinsically fail-safe and avoids a potential failure mechanism and maintenance issue. The lack of a valve improves flexibility in mounting the exchanger and routing pipes. This can reduce the overall reformer volume and can make production of the proposed in-line reformer design easier. The VCHP exchanger can be designed to have a lower pressure drop than the valve-based exchanger since bypass flow around the exchanger is no longer necessary.

II. VCHP Heat Exchanger Design And Modeling

The basis for the work was a 50 kWe system that requires a 4 kW heat exchanger. Synthesis gas at 78 kg/hr and 515°C rejects heat to superheated steam at 28.6 kg/hr and 165°C. The minimum gas flow rates could range from 15% -25% of the maximum flow rates, for a turndown ratio of between 4:1 and 6.7:1. The goal is to passively maintain the temperature of the synthesis gas stream at 415°C ±30°C regardless of changes in either the inlet flow rates or the inlet temperatures. The enthalpy of the superheated steam is to be used elsewhere, where its temperature is not as immediately critical. Since the ultimate goal is a 500 kWe system, this design should be scaleable or modular to allow expansion to larger designs. As well as achieving adequate thermal performance, the resulting exchanger should be optimized for mass and volume.

Design of the exchanger was an iterative process that started with the design of a single heat pipe then progressed to the entire exchanger. Heat pipe design consisted of working fluid selection, reservoir design, then scoping calculations to show the capability of various fin configurations. That information was then folded into a steady state and transient model of a heat exchanger. The exchanger model considered the changing fluid temperatures at each individual VCHP in the exchanger as well as transient effects based on specific heat of representative components. The results of both the VCHP and the heat exchanger modeling work are presented in the following sections. Included are a description of the design method, a discussion of the design trades, and some performance predictions for the final design of both the VCHP and the heat exchanger.

A. VCHP Design and Modeling

Design of the heat pipe began with selection of working fluid and envelope material, then proceeded to wick selection, heat pipe sizing, and fin design. Based on the operating temperature range, cesium was selected as the working fluid. Monel was selected as the primary envelope material since sea water was a potential coolant. Stainless steel was considered as a backup material if fresh water was to be the coolant due to its its lower cost. A coarse powder metal wick was selected to improve heat flux capability and to guard against local dryout at the upstream side of the evaporator. Initial scoping calculations showed that each pipe would carry approximately 250 W at full capacity. An inner diameter of ½" was selected to provide margin against wick dryout and sonic limit. CFD was used to establish heat transfer coefficient and pressure drop for a variety of fin configurations. A series of cases were run with varying fin thickness and spacing. Each case was checked at several flow conditions, including velocity and gas composition. A typical CFD result is show in Figure 5. It shows the synthesis gas temperature profile as it flows past an individual circular fin. Flow is vertical from the bottom, and the average gas temperature was reduced by about 11°C. Based on this CFD work, it was found that a suitable fin was 1" od x 1/8" thick with a 1/8" gap between fins. That kept the fin efficiency high, the heat transfer coefficient high, and the pressure drop low.

Placement and sizing of the non-condensable gas reservoir was considered next. The reservoir could be placed in the hot stream, cold stream, in the heat pipe, or kept at a constant temperature. After looking at the process control affects each position would have, it was determined that only keeping the reservoir at constant temperature (outside the heat exchanger) would provide reliable exchanger outlet temperature control. All of the other positions provide unstable control for certain process changes. For instance, if the reservoir were in the hot stream and both flow rates were increased proportionally, the heat transfer coefficient would go up less than would be required to maintain the temperatures (assuming the heat transfer coefficient goes by flow rate to a power less than 1.) The temperatures close to the inlet would start to rise as would the temperature of the reservoir. As the temperature in the reservoir rose, so would its pressure, blanketing off more of the condenser and lowering the amount of heat transferred (although more heat transfer is required.) Other reservoir positions have similar instabilities with changes in certain process conditions; therefore, keeping the reservoir at constant temperature outside of the heat exchanger was selected for this application.

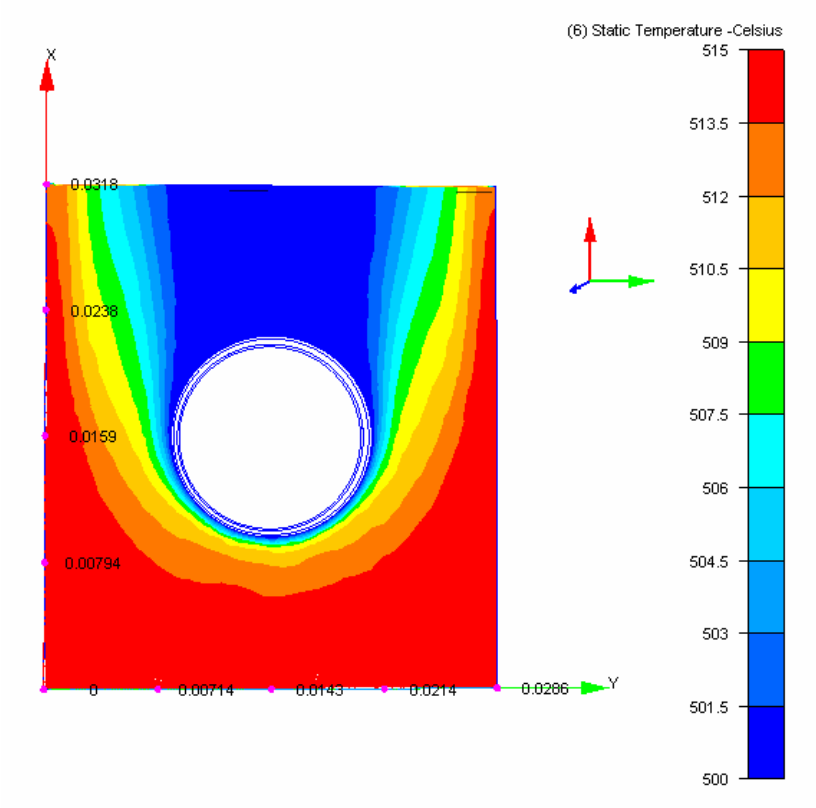

Figure 5: CFD Prediction of Synthesis Gas Temperature Flowing Through a Fin Gap

Equations 1 and 2 describe the energy balance and pressure balance on the heat pipe. They are solved simultaneously to find the heat pipe temperature and the location of the vapor/non-condensable interface location as a function of the heat transfer coefficients and local temperatures. The thermal resistance of the working fluid in the heat pipe is negligible and not accounted for, however the overall thermal resistance of the heat pipe can change, and does so as the exposed area of the condenser, $A_{2,}$ changes. The energy balance is described as

$$h_1 A_1 (T_{HP} - T_1) = h_2 A_2 (T_2 - T_{HP}) \quad (1)$$

where A_1 is the effective condenser area and A_2 is area that is not covered by non-condensable gas. The pressure balance is

$$P_{Sat}(T_{HP}) = \frac{n_{ncg} R T_{ncg}}{V_R + V_c} \quad (2)$$

where V_c is the volume of noncondensable gas in the reservoir.

A plot of gas front displacement versus heat pipe temperature and heat pipe power versus synthesis gas temperature for the chosen VCHP design is shown in Figure 6. The length of the condenser sets the maximum heat transfer rate. For this initial design the heat transfer rate was assumed to be zero for a fully blocked condenser. This assumption ignores second-order effects such as conduction up the heat pipe walls and the effect of diffusion at the vapor/NCG interface. The amount of non-condensable gas in the reservoir relative to the reservoir size was the most critical factor in picking the set point. The volume of the reservoir was chosen so it exceeded the maximum volume of gas in the condenser at all times. This was done for two reasons. The pressure provided by the non-condensable gas should be insensitive to the amount in the reservoir; as it must dominate the denominator in Equation 4. Also, the model does not currently account for the fact the non-condensable gas in the condenser will not be at the temperature of the reservoir, but that of the condenser. However, if the reservoir is larger than the condenser, then this is only a second order effect.

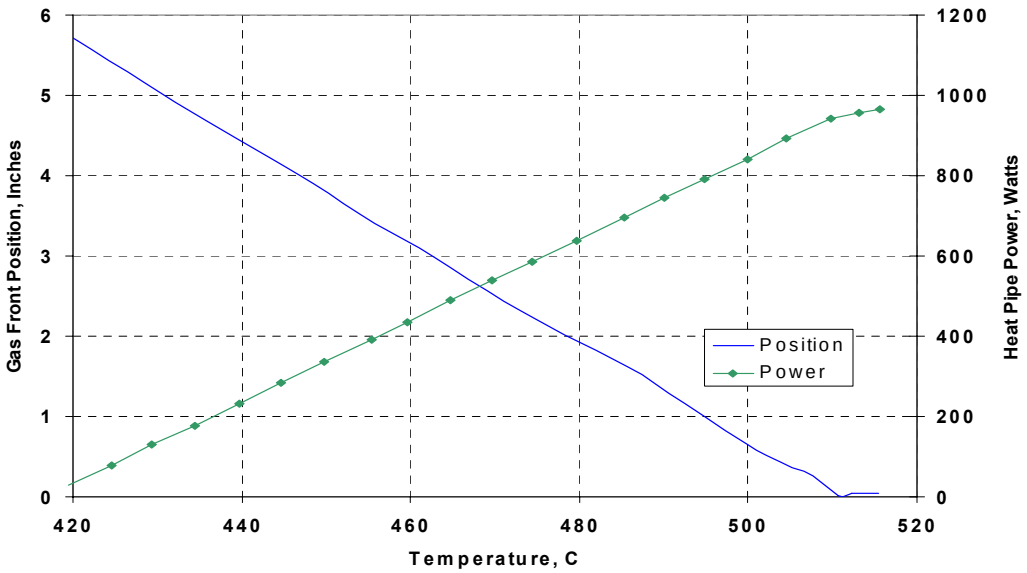

Figure 6: Location of non-condensable gas/vapor interface and heat pipe power for a single VCHP as a function of synthesis gas temperature temperature. 0" signifies that condenser is fully open; 6" means fuly blocked off.

B. Heat Exchanger Modeling and Design

The thermal performance of a simple VCHP exchanger was modeled. The conceptual design for the VCHP heat exchanger was shown previously in Figure 4. To summarize, it consists of one or more finned heat pipes that are mounted perpendicularly through a separator plate or tube sheet. The tube sheet separates the two gas streams. The heat pipes and fins transfer heat between the streams without allowing them to mix. The heat pipe evaporator is located below the condenser which allows condensate return in the heat pipe to be assisted by gravity. The gas and coolant streams flow counter-currently to minimize the overall size of the heat exchanger. The design analyzed in this case has been limited to a single linear array rather than a tube bank. Entry and exit losses were ignored as were potential flow distribution non-uniformities at the interface of the connecting nozzles and the exchanger body.

The behavior of the exchanger is governed by Equations 3 and 4, which describe the time-dependent energy balance for each fluid stream in a counter-current heat exchanger.[8,9] A computer program was written that discretized and integrated these two equations over all of the heat pipes of the baseline exchanger. The program considered local changes in the overall heat transfer coefficient based on local fluid property values, flow rates, and heat pipe thermal conductance. The program could compute time dependent axial temperature profiles based on user-determined changes in flow rates and inlet temperatures to the two fluid streams, which can be useful in predicting process control responses.

$$\frac{\partial T_1}{\partial t} = -v_1 \frac{\partial T_1}{\partial x} - \frac{U}{(\rho C_P H)_1}(T_1 - T_2) \tag{3}$$

$$\frac{\partial T_2}{\partial t} = -v_2 \frac{\partial T_2}{\partial x} + \frac{U}{(\rho C_P H)_2}(T_1 - T_2) \tag{4}$$

An exchanger composed of 24 VCHPs was modeled. Based on a capability of 250 watts per VCHP, this gave a theoretical exchanger capacity of 6 kW, or 50% greater than the design requirement. That provided performance margin to allow for construction errors such as bypass flow; fouling during operation; and modeling uncertainty. The total exchanger length was therefore 24 inches based on heat pipes with 1" diameter fins. Although the exchanger was modeled as a linear array it could be folded into a serpentine later during construction. The resulting folded exchanger package was 12" tall x 12.5" deep x 6" wide including partitions and sidewalls.

The steady-state temperature distribution through the heat exchanger at two different operating conditions is shown in Figure 7. The solid lines correspond to both streams at maximum flow (78 and 28.6 kg/hr) and normal operating temperatures; the dotted lines show the distribution at 15% of their maximum flow rate. The synthesis gas comes in at the 0" location while the steam enters at the 24" location. The outlet temperatures for the synthesis gas are 416°C for both full flow and 15% of full flow rate.

The performance predictions show that the VCHP-HX maintains the synthesis gas outlet temperature within the design range over wide ranges of flow conditions. The variation in outlet temperature was less than 1°C for a turndown ratio of 6.7:1, which exceeds the stated design goal of ±30°C for a 5:1 turndown ratio. A similar result was obtained for several combinations of turndown ratios. A worst-case condition of a 50% decrease in steam flow rate maintaining synthesis gas at the maximum flow rate was modeled. Normally the synthesis gas stream would encounter a large increase in temperature, as the steam side would transfer heat less effectively as the heat transfer coefficient falls, and effectively because it loses driving force as its thermal capacitance would be less. For this, one of the worst possible cases, the outlet temperature of the synthesis gas remained within 19°C of the set point.

The plot of Figure 7 also shows the differentiating features of the VCHP heat exchanger versus standard counter-current heat exchangers. Normally the temperature distributions form parallel lines when the streams are of near equivalent thermal capacitance or with one stream asymptotically approaching another stream of greater thermal capacitance. The curves for the VCHP are different. Since the non-condensable gas shuts off the condenser as the temperature of the synthesis gas approaches its designed set point, the heat transfer rate decreases as the gas cools. This can be seen by the decreasing slope of the synthesis gas temperature curve as it approaches the outlet. Where the temperature is largest, the slopes of both curves are the greatest, signifying the greatest heat transfer. Where the lines are flat that portion of the heat exchanger is essentially inactive.

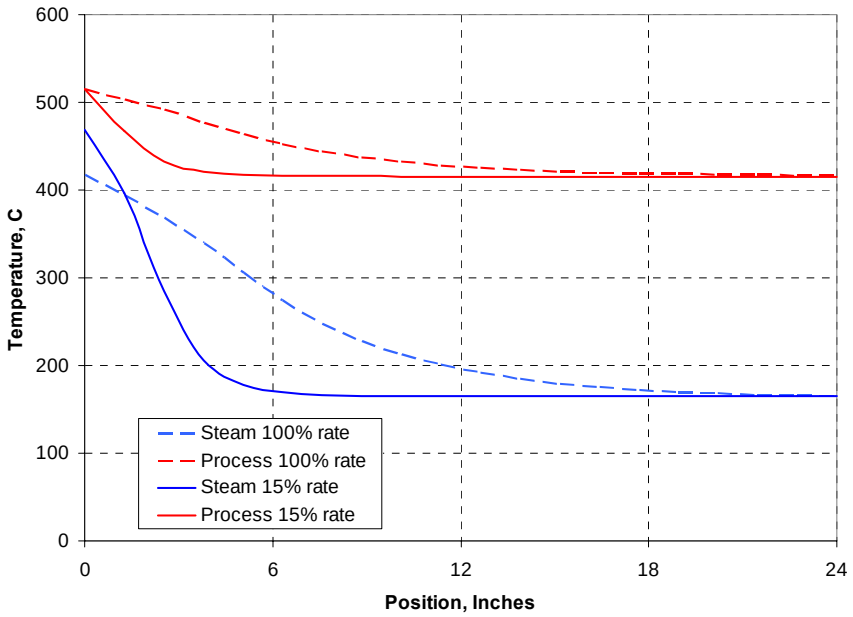

Figure 7: Steady-state axial temperature predictions at maximum flow rate and 15% of maximum flow rate. The predictions show that the VCHP-HX design exceeds the goal of less than ±30°C variation at a turndown ratio of 5:1.

III. Component Demonstration

Both a single VCHP and a heat exchanger consisting of a linear array of six VCHPs were constructed and tested. The single VCHP had a stainless steel envelope and used cesium as a working fluid. It operated at the temperatures expected in the actual fuel cell reformer heat exchanger. This device validated the heat pipe design equations and showed that the gas front moved into the condenser as required. The linear array used copper/water VCHPs and

operated at lower temperatures. This array was used to validate the heat exchanger design equations and to show the ability to control the outlet gas temperature. Both tests and the test results are described below.

A. Stainless Steel/Cesium VCHP

A single stainless steel/cesium VCHP was fabricated and tested to show that the position of the gas front moved as predicted by the mathematical model. The test article is shown below as Figure 8. This VCHP has the same geometry as the VCHP to be used in the actual fuel cell heat exchanger design. The evaporator and condenser were both 6 inches long. The fins were 1" diameter x 1/8" thick with a 1/8" gap between each fin. A larger fin at the center simulated the tube sheet and served as an attach point for a holding fixture. The reservoir was 4" long. The entire heat pipe including fins and reservoir was machined from a single bar to eliminate the contact resistance between the fin root and the heat pipe body. A sintered stainless steel powder metal wick covered the heat pipe and reservoir walls. After fabrication the heat pipe was charged with cesium working fluid then the reservoir was filled with Argon control gas.

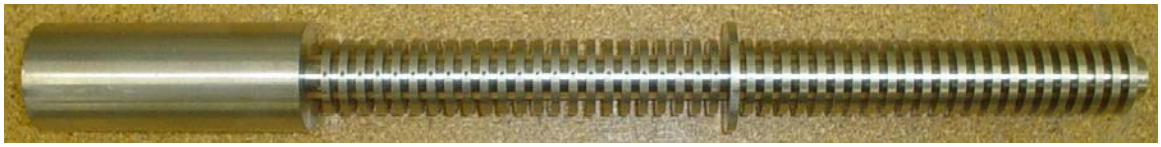

Figure 8: Stainless Steel VCHP with 6" evaporator and condenser, 4" reservoir, and 1/8" thick integral fins.

The heat pipe and test apparatus are shown in Figure 9 at right. The heat pipe was mounted vertically. A cylindrical band heater was clamped to the heat pipe evaporator fins. The condenser was cooled by a combination of natural convection and radiation to the room. An array of type K thermocouples was embedded in holes drilled in each of the condenser fins and in several of the evaporator fins. Vapor temperature was measured by a thermocouple inserted into a thermowell that protruded into the vapor space from the evaporator end cap.

The objective of the test was to measure the location of the non-condensable gas/vapor interface as a function of temperature and to compare the result with theoretical predictions. The heat pipe temperature was increased until the condenser was fully open as shown by a lack of a temperature gradient in the condenser. The heat pipe power was then turned off. As the heat pipe cooled the condenser thermocouples and the vapor temperature were monitored so the position of the interface could be determined as a function of vapor temperature. The results of the testing are summarized in Figure 10, which shows the actual and predicted non-condensable gas front locations as a function of temperature. The plot shows good agreement between the experimental results and the model predictions.

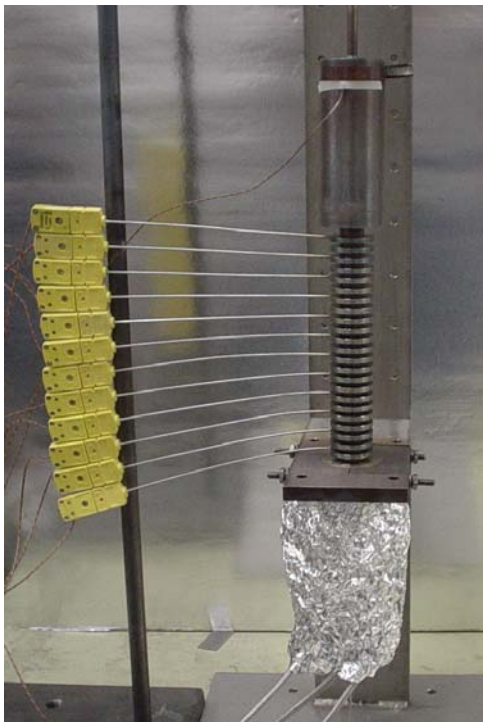

Figure 9: Stainless Steel/Cesium VCHP test apparatus.

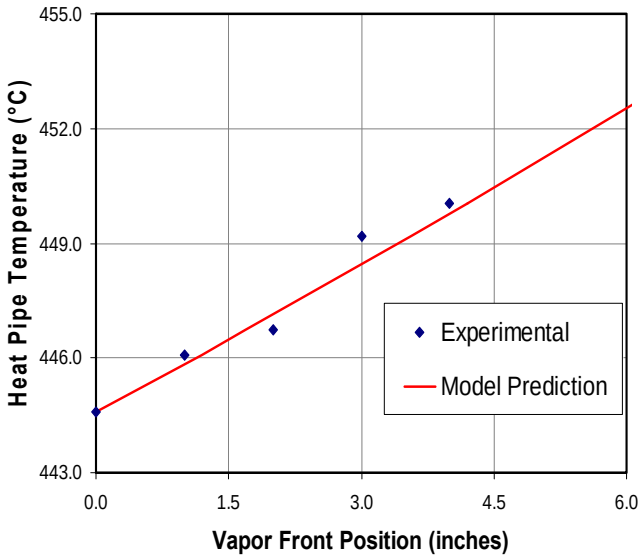

Figure 10. Vapor front position versus heat pipe temperature showing good agreement between experimental results and model predictions.

B. VCHP Heat Exchanger

A heat exchanger segment consisting of a linear array of six VCHPs was fabricated and tested. The VCHPs were made of copper, had screen wicks, and used water working fluid. This allowed operation at lower temperatures and greatly simplified construction and testing. The VCHPs were otherwise identical in size and shape to the cesium VCHP described previously. Counter-flowing air was the heat exchange fluid on each side of the exchanger.

Figure 11 is a schematic of the test setup. Air at ambient conditions will be raised to approximately 150°C by an electrical preheater and subsequently cooled to 125°C as it flows over the lower half of the exchanger. That heat is rejected to a counter-current stream of ambient air flowing over the top half of the exchanger. Instrumentation consisted of thermocouples to measure the temperature at the inlet and outlet of each stream and a thermocouple inserted into a thermowell in the evaporator of each VCHP. Figure 11 shows the actual exchanger under test. The preheater is visible on the lower left port of the exchanger as are the four thermocouples used to measure the temperature of each fluid stream.

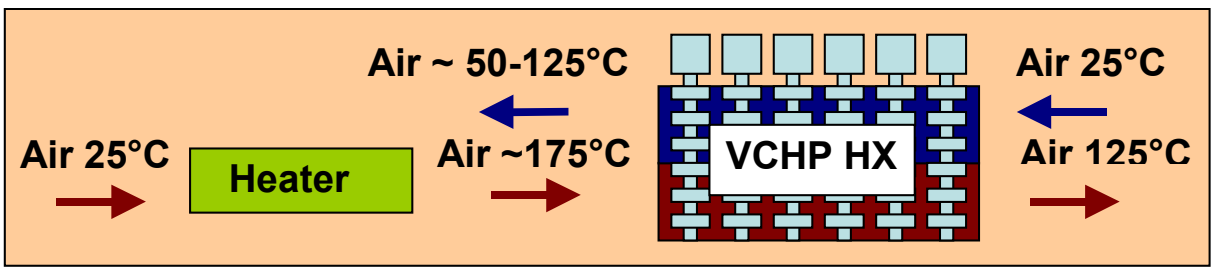

Figure 11. Schematic of Test Setup for Copper/Water VCHP Heat Exchanger

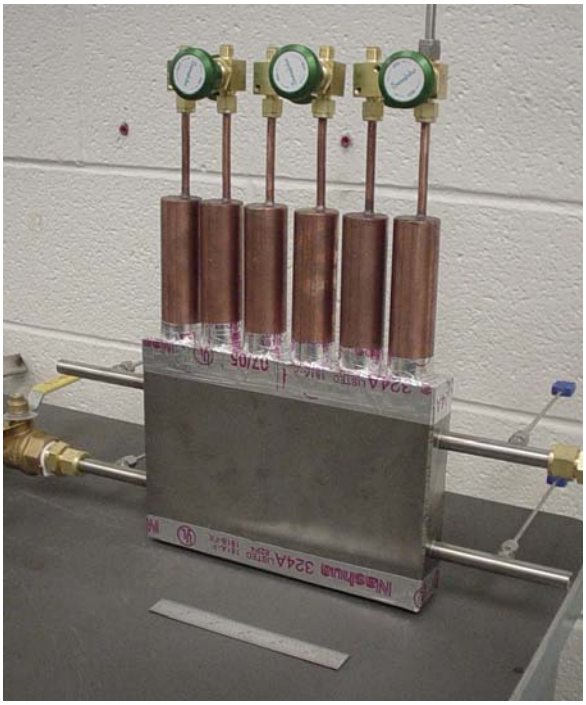

Figure 12. Copper/Water VCHP Heat Exchanger

Prior to filling the VCHP reservoirs with non-condensible gas the test article was operated as a conventional heat exchanger. This allowed measurement of the heat transfer coefficient and comparison with CFD predictions. Gas flow was counter-current with identical flow rates for each stream. Measurements were made at several discrete flow rates. Using the effectiveness-NTU method, the heat transfer coeffcient was calculated at each flow rate. Since the geometries and flow rates of the hot and cold side are the same, the heat transfer coefficients on each side were the same which resulted in an equation to solve for the heat transfer coefficient from the overall heat transfer coefficient. The measured heat transfer coefficient measurements are shown in Figure 13 along with two different CFD predictions. The higher of the two CFD predictions assumed no bypass flow around the VCHP. The lower prediction assumed a 1/16" gap between the VCHP fins and the exchanger wall. The measured values fell along the lower line, which showed that there was some bypass flow around the fins in the actual exchanger and that the bypass flow resulted in a decrease of greater than 20% in thermal performance.

The VCHPs were then charged with non-condensable gas and the heat exchanger thermal resistance measured at a range of flow rates and inlet temperatures. The results are shown in Figure 14, which shows the heat exchanger thermal resistance versus the difference between the inlet hot stream temperature and the set point of the hot stream outlet temperature. Also shown are the theoretical performance predictions for the exchanger with and without gas loading. The actual exchanger performance fell between the two curves. The exchanger did control temperature but not as much as predicted. The primary reason for this was the conductivity of the copper envelope. It allowed a substantial amount of heat to leak through the VCHP even though the gas was fully blocking the condenser. The actual VCHP will be made of stainless steel. With less than $1/20^{th}$ of the conductivity of copper, the heat leak through the heat pipe envelope will be significantly reduced and performance will more closely approach the ideal VCHP performance.

IV. Conclusions

A Variable Conductance Heat Pipe Heat Exchanger (VCHP-HX) has been shown to be a viable means of providing passive thermal control for fuel cell reformers. A single high temperature alkali metal VCHP was designed, including the fins and control gas reservoir. CFD analysis was used to predict heat transfer coefficients and pressure drops of the fins. The VCHP model was used as input for a second model that predicted VCHP-HX performance as a function of hot and cold stream flow rates, hot and cold stream inlet temperatures, and various flow stream physical properties. A single stainless steel/cesium VCHP was constructed. Testing showed that it corresponded closely to the expected performance based on the design calculations. An exchanger based on a linear array of six copper/water heat pipes was constructed. It matched closely the expected performance based on its design calculations, and it demonstrated the ability of a VCHP-HX to passively control the outlet temperature of the hot gas stream over a wide range of turndown conditions.

Future work will lead to the construction and test of a full-scale heat exchanger. The envelopes will be of stainless steel since seawater compatibility is no longer required. Inconel will be considered if hydrogen permeation becomes a problem. The fins will be eliminated as they added little usable heat transfer area in comparison with their added mass. The full-scale exchanger will be integrated into a land-based fuel cell test bed and tested for steady state and transient response.

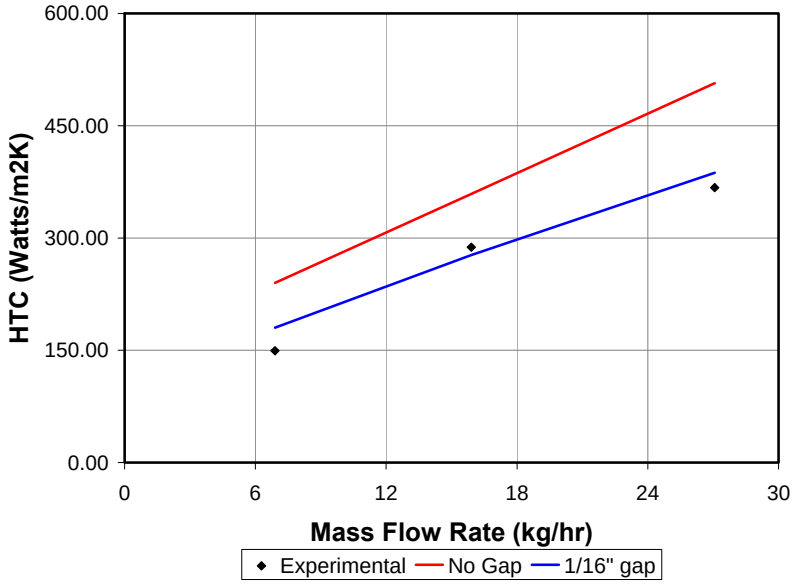

Figure 13: Experimental heat transfer results versus CFD modeling predictions for air flowing over fins used in the copper water heat exchanger.

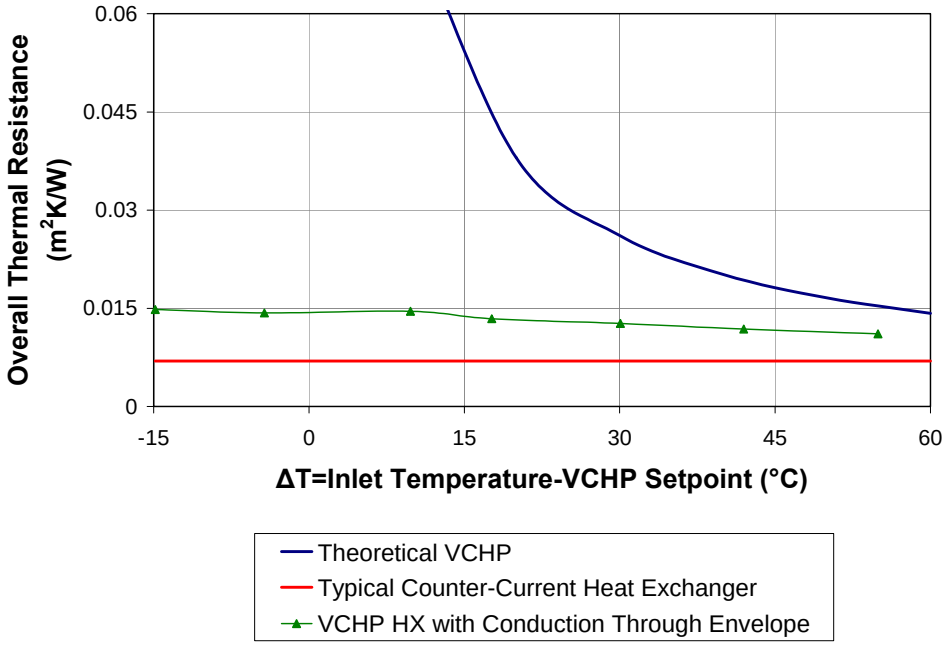

Figure 14: Predicted Thermal Resistance of VCHP Heat Exchanger and Heat Exchanger with No Gas Loading, and Measured Thermal Resistance of 6-Heat Pipe Copper/Water VCHP Heat Exchanger.

Acknowledgments

This material is based upon work sponsored by the Office of Naval Research under Naval Surface Warfare Center contract number N65538-05-M-0139. Mr. Donald Hoffman was the technical monitor. Any opinions, findings, and conclusions and recommendations expressed in this material are those of the authors and do not necessarily reflect the views of the Naval Surface Warfare Center or the Office of Naval Research. The authors thank David Glatfelter of ACT for fabricating and testing the heat pipes and VCHPs.

References

[1]S.W. Scoles M.A. Perna, Naval Distillate Reforming for Navy Ship Service Applications, *Presented at the 2000 Fuel Cell Seminar*, MTI 00-28, Portland, Oregon, 2000.

[2]Hoffman, D., Nickens, A., Skruch, H., "Naval Shipboard Fuel Cell Program," *Shipbuilding Technologies,* Biloxi, MS, 2003.

[3]Privette, R.M., Flynn, T.J., Perna, M.A., Kneidel K.E., King, D.L., Cooper, M. "Compact Fuel Processor for Fuel Cell-Powered Vehicles*," DOE/EPRI/GRI Fuel Cell Technology Review Conference,* MTI 00-10, Chicago, Illinois, 1999.

[4]Dunn, P. D. and Reay, D. A., *Heat Pipes*, 4th ed. Pergamon, New York, 1994, Chaps. 1, 6.

[5]Marcus, B.D., "Theory and Design of Variable Conductance Heat Pipes: Control Techniques," Research Report 2, Ames Research Center, National Aeronautics and Space Administration. 13111-6027-R0-00.

[6]Marcus, B. D., "Heat Pipes: Control Techniques," Report 2, NASA Contract No. NAS2-5503, 1971.

[7]Bienert, W., "Heat Pipes for Temperature Control," *Proceedings of the Fourth Intersociety Energy Conversion Conference*, Wash., DC, 1969, pp. 1033-1041.

[8]Chapman, A. J., *Heat Transfer*, 4th ed. MacMillan Publishing Company, New York, 1984, Chap. 12.

[9]Deen, W. *Analysis of Transport Phenomena,* 1st ed. Oxford University Press, New York, 1998, pp. 40-45.